JOURNAL OF PROPULSION AND POWER
Vol. 10, No. 4, July–Aug. 1994

Lag Model for Turbulent Boundary Layers over Rough Bleed Surfaces

J. Lee,* M. L. Sloan,* and G. C. Paynter†
Boeing Commercial Airplane Group, Seattle, Washington 98124

Boundary-layer mass removal (bleed) through spanwise bands of holes on a surface is used to prevent or control separation and to stabilize the normal shock in supersonic inlets. The addition of a transport equation lag relationship for eddy viscosity to the rough wall algebraic turbulence model of Cebeci and Chang was found to improve agreement between predicted and measured mean velocity distributions downstream of a bleed band. The model was demonstrated for a range of bleed configurations, bleed rates, and local freestream Mach numbers. In addition, the model was applied to the boundary-layer development over acoustic lining materials for the inlets and nozzles of commercial aircraft. The model was found to yield accurate results for integral boundary-layer properties unless there was a strong adverse pressure gradient.

Nomenclature

A = constant (26.0) in van Driest's damping function, Eq. (3)
k_s = equivalent sand-grain roughness height
k_s^+ = roughness Reynolds number, $k_s u_\tau/\nu$
k_2 = constant (0.02) in outer layer eddy viscosity model, Eq. (4)
k_3 = constant (0.5) in the lag model, Eq. (7)
l = length scale
m_{bl} = bleed mass flow rate
p = static pressure
R = augmented mixing length due to surface roughness effect
Re = Reynolds number
u, v = velocity components in the streamwise and the normal to surface directions
u_τ = frictional velocity
x, y = coordinates in the streamwise and the normal to boundary-layer surface directions
Γ = intermittency factor in Eq. (4), $0 < \Gamma < 1$
δ^* = displacement thickness
θ = momentum thickness
$\varkappa$ = von Karman constant, 0.40, Eq. (3)
μ = viscosity
ρ = density
ν = kinematic viscosity of the fluid

Subscripts
e = outer region of boundary layer
eq = equilibrium turbulent flow
t = turbulent flow

Superscripts
$'$ = fluctuating turbulent quantity
$+$ = quantity normalized by ν/u_τ

Introduction

BOUNDARY-LAYER control is used to improve the performance and stability of engine inlets for supersonic aircraft. High total-pressure recovery, low distortion, and normal-shock stability (in a mixed-compression inlet) are achieved through the use of boundary-layer mass removal or bleed on an inlet wall for boundary-layer control. A schematic of a supersonic inlet with the locations of bleed bands is illustrated in Fig. 1. Bleed is typically removed through the surface through tightly spaced transverse bands of holes as shown in Fig. 2, located ahead of regions of adverse pressure gradient such as shock/boundary-layer interaction.

Bleed can, however, also increase the growth rate of the boundary layer, reduce the near-wall streamwise velocity, and increase the chance for a boundary-layer separation. This negative effect of bleed on the growth of a boundary layer has been termed the bleed roughness effect. Bleed roughness is a function of the local freestream Mach number, the local boundary-layer properties, the bleed configuration, and the bleed rate. The inlet designer wishes to select a bleed configuration for which the positive effect of mass removal is obtained with minimum negative effect of bleed roughness.

The rapid advances in the available computer memory and speed have led to increased interest in the use of Navier-Stokes (NS) analysis for inlet design support. Accurate simulation of an inlet flow requires accurate simulation of the boundary-layer development, including the effects of bleed.

While NS analysis has been used to predict the flow through individual bleed holes, this is impractical in the context of an inlet design because of the size and complexity of the grid that would be required. If NS analysis is to be used for inlet design, a simulation of the effect of bleed on the boundary layer is needed that does not require a local grid adequate to resolve the flow through each bleed hole. As noted in Ref. 1, the bleed-simulation model should relate changes in the boundary-layer velocity distribution across a bleed band to the bleed hole configuration, bleed flow rate, and local freestream Mach number, without increasing the grid required to resolve the boundary layer.

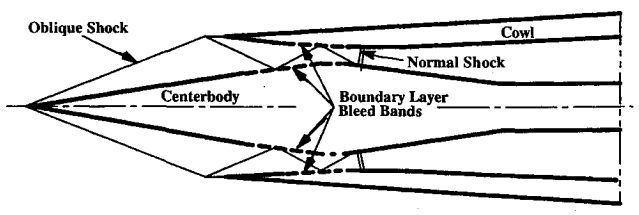

Fig. 1 Schematic diagram of a supersonic inlet and the locations of boundary-layer bleed bands.

Presented as Paper 93-2988 at the AIAA 24th Fluid Dynamics Conference, Orlando, FL, July 6–9, 1993; received Aug. 2, 1993; revision received Nov. 30, 1993; accepted for publication Dec. 9, 1993.

*Principal Engineer. Member AIAA.
†Senior Principal Engineer. Associate Fellow AIAA.

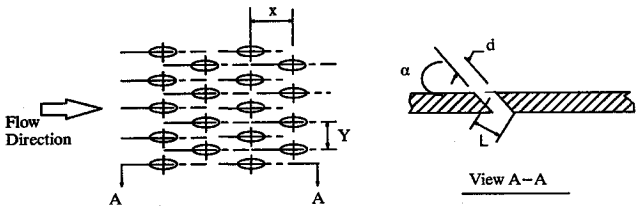

Fig. 2 Typical bleed band configuration.

Paynter et al.[1] applied the algebraic turbulence model of Cebeci and Chang[2] to the modeling of bleed roughness. This model increases the turbulence length scale in the inner layer of the boundary layer as a function of an equivalent sand-grain roughness and local flow properties. For a given bleed geometry and bleed rate, a roughness value was determined from available experimental data by varying the roughness specified for the surface over the bleed region until the computed velocity profile immediately downstream of the bleed band matched the experimental profile in the log law region. The model was also applied to the prediction of boundary-layer growth over acoustic linings used in the inlets and nozzles of commercial aircraft for noise suppression.

The Cebeci-Chang roughness model was found to be accurate for the near-wall reduction in streamwise velocity that was observed downstream of a bleed band, but the overall shape of the predicted mean velocity profile was not in good agreement with the measured profile for cases with high bleed. One possible explanation for this was that a history effect is important and that the Cebeci-Chang algebraic turbulence model neglects this effect. In an attempt to include this effect, a transport equation lag relationship for eddy viscosity developed for impermeable walls was tried. While the shape of the predicted mean velocity distributions downstream of a bleed band was different with the impermeable wall lag model, agreement with the experimental data was generally no better than with the algebraic model.

With bleed, streamlines near the wall within the boundary layer over a bleed band are at a significant angle to the wall. Eventually, it was realized that the lag model developed for impermeable walls would convect the eddy viscosity parallel to the wall and that this was incorrect for cases with bleed. The lag model was reformulated to correct this deficiency. This article proposes a transport equation model extension for the eddy viscosity for predicting the boundary-layer development over surfaces with boundary-layer bleed. Results achieved with the reformulated lag model are reported through comparisons with experimental data at Mach 1.6 for bleed configurations with 20- and 90-deg holes, and for bleed rates between 0–12% of the boundary-layer mass flux. Results are also reported for the boundary-layer growth over acoustic paneling through comparisons of predicted and measured integral properties along the paneling.

Approach

Starting with the algebraic turbulence model of Cebeci and Chang, a simple transport equation model for eddy viscosity was formulated to include the effects of bleed on the convection of eddy viscosity. The model was implemented in the boundary-layer method of Reyhner.[3] Assuming that the bleed rate and the roughness are constant over a bleed band (generally only several boundary-layer thicknesses in streamwise extent) and zero downstream of a bleed band, roughness values were determined for the bleed cases through comparisons between computed and measured mean velocity distributions at a profile station downstream of a bleed band. The model was also evaluated for acoustic paneling using experimentally derived equivalent sand-grain roughness values through comparisons of predicted and measured integral properties over the acoustic surface.

Equilibrium Turbulence Model

In the mixing length hypothesis, the turbulent viscosity is assumed to be

$$\mu_t = \rho l u' \tag{1}$$

For a smooth wall, in the near-wall region, the velocity scale is

$$u' = l \left| \frac{du}{dy} \right| \tag{2}$$

The van Driest's length scale formulation for the inner layer is

$$l = \kappa y\{1.0 - \exp[-(y^+/A^+)]\}$$

For a rough wall, the Cebeci-Chang assumed a modified length scale in the inner layer

$$l = \kappa(y + R)\{1.0 - \exp[-(y + R)^+/A^+]\} \tag{3}$$

The equilibrium eddy viscosity in the inner layer, μ_{teq}, is computed from Eqs. (1–3).

In the outer region of the boundary layer a Clauser[4] formulation was used:

$$\mu_{te} = k_2 \rho u_e \delta^* \Gamma \tag{4}$$

In computing the boundary-layer development with the equilibrium model, the eddy viscosity at each point across the layer is computed using both the inner layer and outer layer formulations. The minimum value at each point is used to compute the local shear stress.

R in Eq. (3) is the increase in mixing length due to surface roughness and is calculated based on the formulation by Rotta[2]:

$$R = 0.9(\nu/u_\tau)[\sqrt{k_s^+} - k_s^+ \exp(-k_s^+/6)] \tag{5}$$

The valid range of the roughness Reynolds number ($k_s^+ = k_s u_\tau/\nu$) in the formula (5) is $4.535 < k_s^+ < 2000$ with the lower bound corresponding to the upper bound for smooth surface. The sequence to calculate the local eddy viscosity during the iterative solution of boundary layer at a given marching station including the surface roughness effect k_s is to calculate Eqs. (5), (3), and (1) in order. All k_s^+ values of the present study were within the valid range ($k_s^+ < 2000$). However, for highly rough surfaces with k_s^+ greater than 2000, new formulations for R and the inner layer eddy viscosity are required. The present scheme of selecting the minimum of the viscosities computed using both the inner layer and outer layer formulations as a turbulent viscosity at a point within a boundary layer may need refinement so that the viscosity calculated with the modified inner layer formulation (3) could be used over the height of the roughness element, although the outer layer eddy viscosity based on Eq. (4) is smaller (for large roughness values).

Reyhner Lag Model

In order to account for history effects for a boundary layer developing over an impermeable surface, Reyhner formulated the lag relationship for eddy viscosity given in Eq. (6) below:

$$\frac{d\mu_t}{dx} = \frac{k_3}{\delta^*}(\mu_{teq} - \mu_t) \tag{6}$$

Eq. (6) can be considered a transport equation for eddy viscosity normalized by the local velocity in the streamwise direction.

Proposed Lag Model

With bleed, the component of velocity normal to the wall is no longer approximately equal to zero. A transport equation formulated to include this effect is as follows:

$$\frac{\partial \rho u \mu_t}{\partial x} + \frac{\partial \rho v \mu_t}{\partial y} = \rho u \frac{k_3}{\delta^*} (\mu_{teq} - \mu_t) \tag{7}$$

The physical meaning of Eq. (7) is that the convective change of the eddy viscosity is equal to the imbalance between the production and dissipation of the local eddy viscosity. Equation (7) can be simplified by eliminating the mass continuity relationship from the left side of the equation, and by division through by u, which gives

$$\frac{\partial \mu_t}{\partial x} + \frac{v}{u} \frac{\partial \mu_t}{\partial y} = \frac{k_3}{\delta^*} (\mu_{teq} - \mu_t) \tag{8}$$

With zero bleed, Eq. (8) reduces to Eq. (6) which was the original Reyhner lag formulation.

The lag model Eq. (8) was solved coupled with the turbulent boundary-layer equations at a given marching station.

The description of the overall governing mathematical equations, the boundary conditions, and the solution procedure to analyze a turbulent boundary-layer flow are not included in this article, because this information is available from Ref. 3, and the objective of the present study was the turbulence modeling including the effects of the boundary-layer mass bleed and the surface roughness. The only additional boundary condition required with the lag model for rough bleed surfaces is the specification of a uniform mass flux normal to bleed surface. With the specification of a nonzero roughness value, the eddy viscosity is greater than zero on the wall. The uniform mass flux was estimated based on a given bleed rate and the porosity and discharge characteristics of a bleed hole configuration.

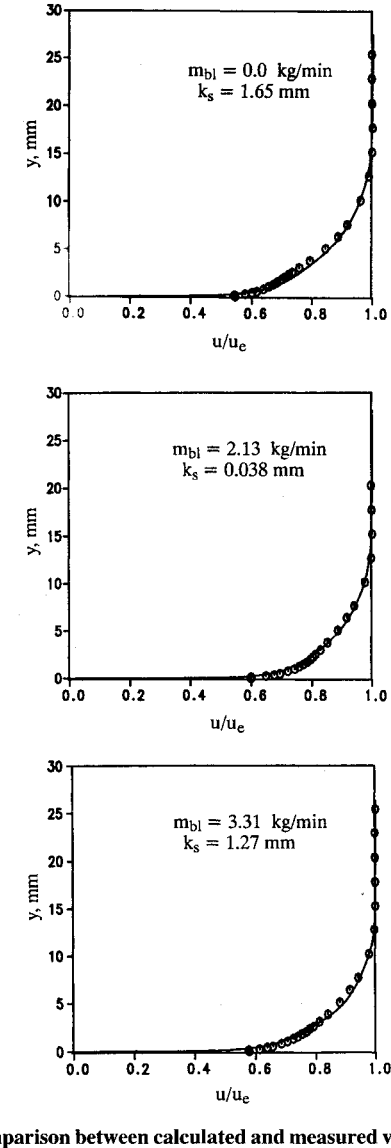

Fig. 3 Comparison between calculated and measured velocity profiles downstream of 20-deg hole bleed surfaces (——: prediction; symbols: experiment).

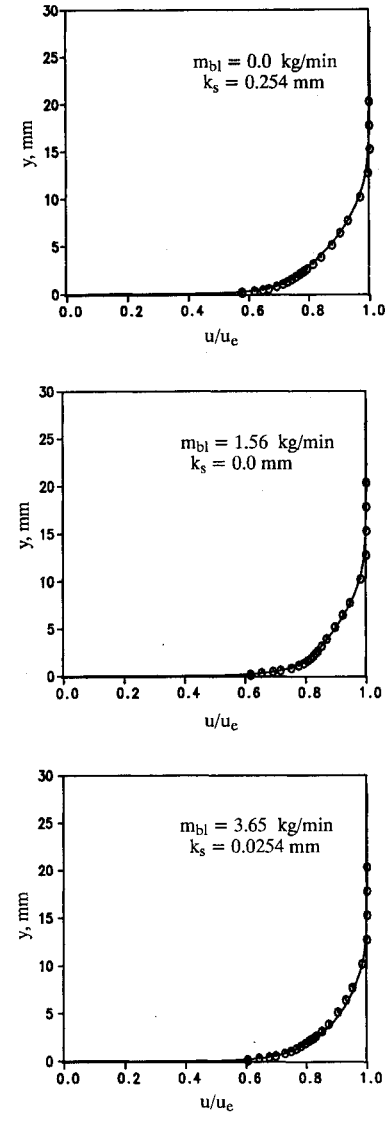

Fig. 4 Comparison between calculated and measured velocity profiles downstream of 90-deg hole bleed surfaces (——: prediction; symbols: experiment).

Results and Discussion

The two-dimensional lag model was evaluated through comparisons between boundary-layer analysis results and available experimental data for the turbulent boundary-layer development over rough bleed surfaces and over a variety of acoustically treated rough surfaces. Discussion of the results follows.

For the boundary-layer calculations reported in this article, computational grids were generated at each marching step using approximately 50 points in the cross-stream direction at each streamwise station. The near-wall y^+ grid value was typically less than 2. Boundary-layer analyses were conducted

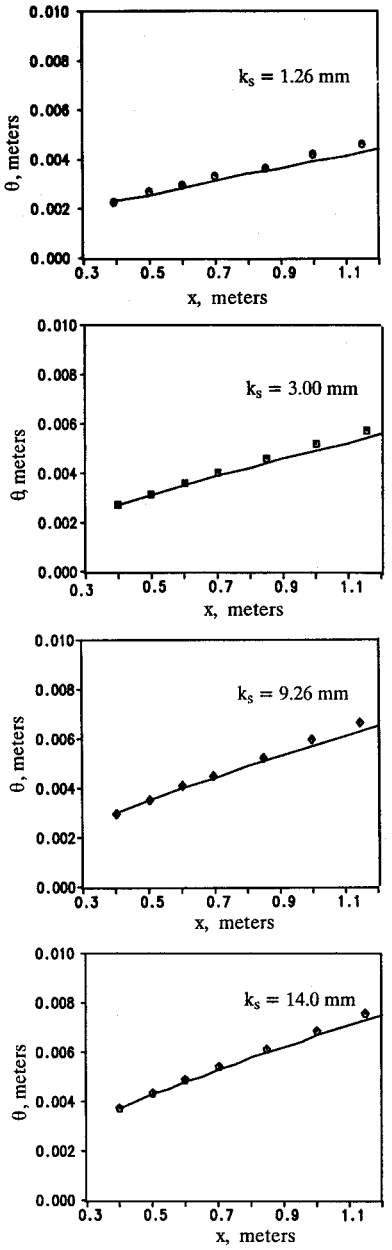

Fig. 5 Comparison between calculated and measured momentum thicknesses (Betterman's data, u_e = 30 m/s; ——: prediction; symbols: experiment).

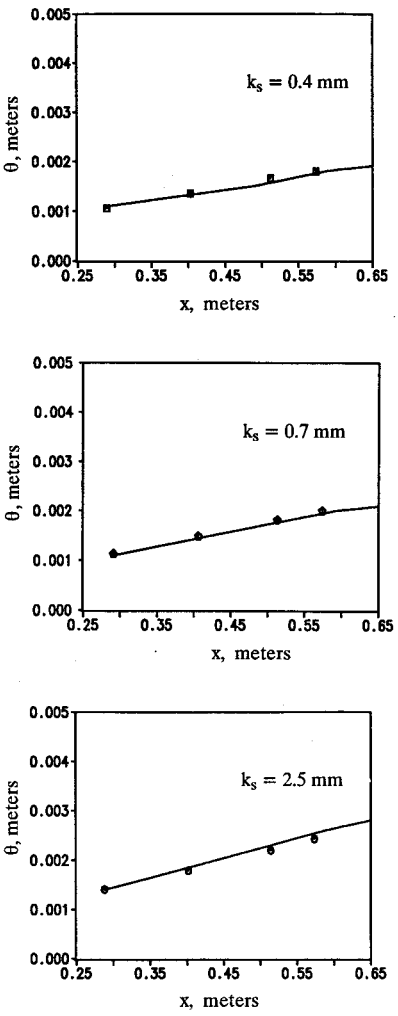

Fig. 6 Comparison between calculated and measured momentum thicknesses (Arndt's data, u_e = 12.3 m/s; ——: prediction; symbols: experiment).

on an engineering workstation, and the run time for a given case was typically less than 1 min.

Boundary-Layer Flow over Rough Bleed Surfaces

The turbulent boundary layers developing over surfaces with 20- and 90-deg bleed hole configurations were considered for the evaluation of the two-dimensional lag model. The hole diameters were 0.1 and 0.2 in. for 20- and 90-deg hole configurations, respectively, and bleed rates between 0 and approximately 12% of the boundary-layer mass flow (just upstream of the bleed band) were considered. The freestream Mach number at the test section was approximately 1.6. In the analysis, the measured velocity profiles were used to initialize the calculation at approximately 2 boundary-layer thicknesses upstream of a bleed band.

In the application of the two-dimensional lag model, an optimum k_3 value of 0.5 was chosen for the empirical constant. This empirical constant value gave the best results for all the bleed hole configurations over the entire allowable bleed flow rate ranges tested in the present study.

The equivalent sand-grain roughness heights for bleed surfaces were determined by varying the equivalent sand-grain roughness height until the predicted streamwise velocity profile matches the measured velocity profile at a velocity profile station at about 5 upstream boundary-layer thicknesses downstream of a bleed band.

Results for the 20-deg bleed hole configuration at bleed rates of 0.0, 2.13, and 3.31 kg/min (approximately 12% of the boundary-layer mass flow) are presented in Fig. 3. The variation of the velocity profile downstream of the bleed band is shown for a range of bleed flow rates. Agreement between predicted and experimental velocity profiles is improved relative to that which was achieved without the lag model.[1]

Without the lag model, the agreement for the shape of the predicted downstream velocity profiles is not as good at any equivalent sand-grain roughness height (see Ref. 1). Consequently, the equivalent sand-grain roughness height representing a bleed surface was sometimes difficult to determine. With the two-dimensional lag model, the shape of the predicted velocity profile could be matched closely with the experimental velocity profile shape to determine an equivalent sand-grain roughness height. The predicted equivalent sand-grain roughness height for the 20-deg bleed surface ranges from 0.038 to 1.65 mm at the medium and zero bleed rates, respectively. The reason why the roughness effect (1.27 mm) becomes important at the higher bleed rate of 3.31 kg/min is not clear.

For the 90-deg bleed hole configurations, the two-dimensional lag model results were also in excellent agreement with

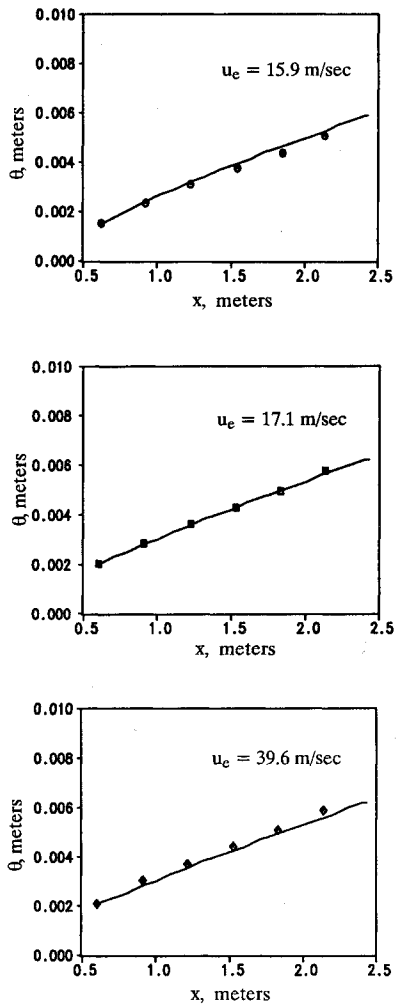

Fig. 7 Comparison between calculated and measured momentum thicknesses (Pimentha et al.'s data, k_s = 0.793 mm; ——: prediction; symbols: experiment).

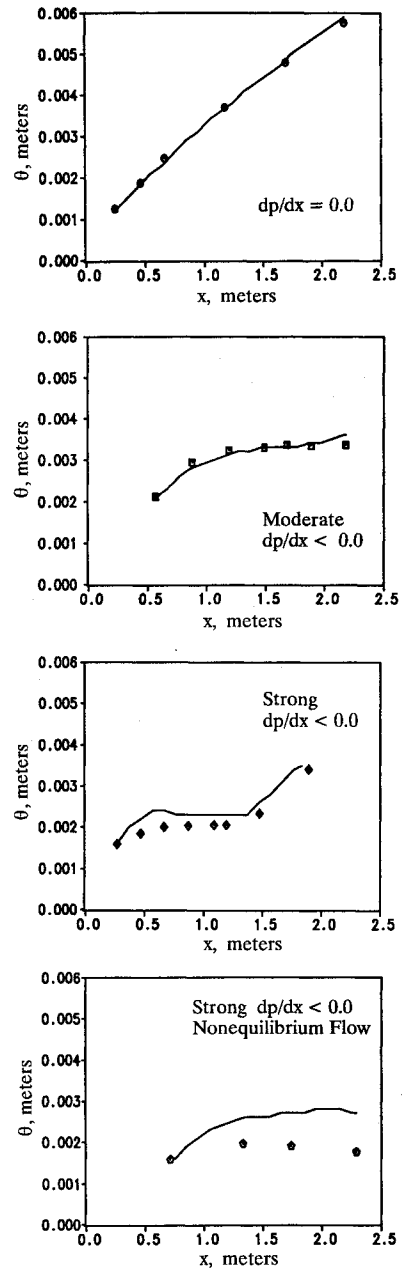

Fig. 8 Comparison between calculated and measured momentum thicknesses (Coleman et al.'s data, u_e = 26.4 m/s, k_s = 0.8 mm; ——: prediction; symbols: experiment).

the measured velocity profiles over a range of bleed rate up to 12% of boundary-layer mass flow as shown in Fig. 4. The predicted equivalent sand-grain roughness heights for the bleed flow rates of 0.0, 1.56, and 3.65 kg/min are 0.254, 0.0, and 0.0254 mm, respectively.

Figures 3 and 4 indicate, first, the bleed roughness effect is a function of bleed flow rate, and, second, the bleed roughness effect for the 90-deg bleed hole is smaller than that for a 20-deg bleed hole surface at the bleed rates shown.

The results presented demonstrate that the two-dimensional lag model improves the shape of predicted boundary-layer velocity profiles relative to what could be obtained with just the algebraic Cebeci-Chang model, particularly in the region close to the surface. The two-dimensional lag model accounts for the nonequilibrium history effect of turbulent eddy motion within the boundary layer over a bleed band and allows eddy viscosity to be transported along streamlines. The effectiveness of the two-dimensional lag model implies that the eddy viscosity distribution over a bleed band is dependent not only on the local eddy viscosity distribution law within the inner layer of the boundary layer, but also on the nonequilibrium transport and decay along a streamline (history effect).

Turbulent Boundary Layer Development over Acoustically Treated Rough Surfaces

The lag model was evaluated for the boundary-layer development over acoustically treated rough surfaces through comparisons between predicted and the experimental data by Betterman, Arndt et al., Pimentha et al., Coleman et al., and Scottron et al. from Ref. 2.

Boundary-layer calculations were started from a experimental velocity profile and used the measured Reynolds number and pressure distribution. The initial velocity profile was estimated from the experimental momentum thickness and the shape factor assuming a turbulent velocity profile. Calculations were carried out over the distance of the experimental test. It is noted that all the calculations were conducted using the equivalent sand-grain roughness heights k_s reported in Ref. 2, where the k_s values were determined using Cebeci and Chang's boundary-layer model. No attempt was made to determine an equivalent sand-grain roughness for the lag model. The momentum thickness which accounts for the cumulative momentum loss in the boundary layer was used as a measure of the prediction.

Figure 5 shows the comparison between predicted and measured momentum thickness growth for the test data by Betterman for the four flat surfaces with the equivalent sand-

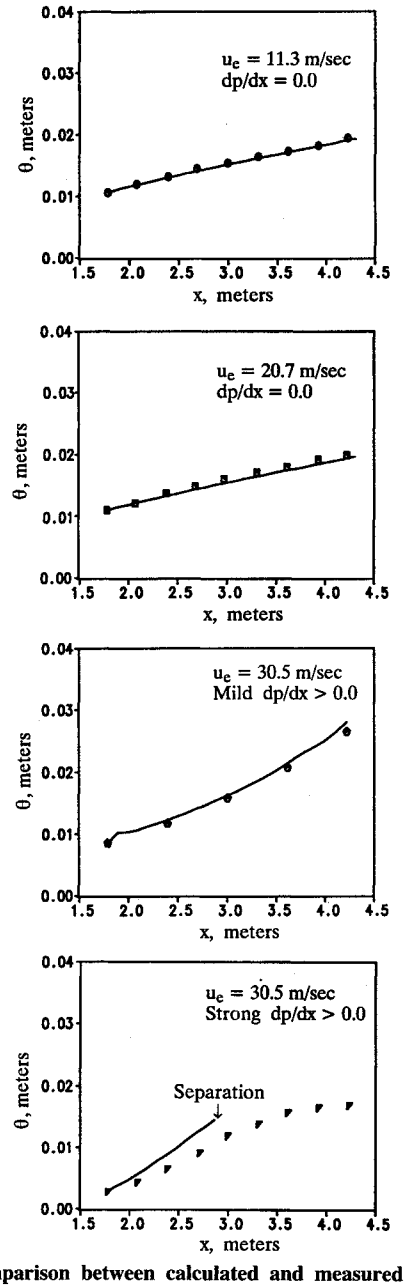

Fig. 9 Comparison between calculated and measured momentum thicknesses (Scottron et al.'s data, k_s = 1.2 mm; ——: prediction; symbols: experiment).

grain roughness heights between 1.26–14.0 mm. The freestream velocity was 30 m/s.

Figure 5 indicates that agreement between predicted and meaured momentum thicknesses over a distance of approximately 1 m is, in general, satisfactory (the measured data was slightly underpredicted). The slight underprediction may be due to the use of a k_s from Cebeci and Chang's boundary-layer model. It is obvious that the prediction would be improved by a slight adjustment of k_s. Another possible source of the discrepancy may be uncertainties introduced when the initial boundary conditions were estimated from the published graphical data.

The comparisons of Arndt's momentum thickness data with the boundary-layer predictions are shown in Fig. 6 for boundary-layer flows over three rough surfaces with triangular grooves. The three different equivalent sand-grain roughness heights based on half the peak-to-peak distance of the grooves are 0.40, 0.70, and 2.5 mm. The Reynolds number was 1.39 $\times$ 10^7. Over the distance of $\frac{1}{2}$ m, the predictions were very satisfactory for all three cases.

The next cases by Pimentha et al. (Fig. 7) and Coleman et al. (Fig. 8) were flows over rough surfaces composed of densely packed spheres of uniform size with a diameter of 1.27 mm. A favorable pressure gradient was applied to both equilibrium and nonequilibrium flows. Pimentha et al. varied the freestream velocity from 16 m/s to 40 m/s at a fixed surface roughness condition (k_s = 0.793 mm). As shown in Fig. 7, the predicted momentum thicknesses are in excellent agreement with the experimental data over a 2-m length for all three velocity conditions. The comparison between the Coleman et al.'s experimental data and the predicted results at a constant freestream velocity of 26.4 m/s are shown in Fig. 8. The boundary-layer predictions for the zero and the strong favorable pressure gradient cases agree very well with the data. However, the test data was overpredicted for the nonequilibrium flow with a strong favorable pressure gradient. Poor prediction was anticipated for the nonequilibrium flow case, because the nonequilibrium flow model was not used for the roughness calculations.

The effect of pressure gradient on the boundary-layer development on rough surfaces were further examined by Scottron and Power's experiment. Their tests were done using a square mesh screen with a fixed surface roughness condition (k_s = 1.2 mm), while different experimental freestream velocity distributions corresponding to different pressure conditions—zero, mild, and strong adverse pressure gradients were considered. The calculated and measured results are compared in Fig. 9. For the zero pressure gradient cases, the predicted momentum thickness variations are in good agreement with the experimental data at the two different velocity conditions as demonstrated through Pimentha et al.'s cases. For the mild adverse pressure gradient case, a good prediction was consistently achieved, whereas the momentum thickness was overpredicted for the strong adverse pressure gradient.

Conclusions

A two-dimensional lag model was added to a compressible, turbulent boundary-layer code, and evaluated using experimental data for the boundary-layer development over rough bleed surfaces and acoustically treated rough surfaces. Based on the evaluation results, the following conclusions can be drawn.

1) The two-dimensional eddy viscosity lag model improved the accuracy of the predicted velocity profile shape downstream of a bleed band. Predicted velocity profiles were in good agreement with the measured data for the 20- and 90-deg bleed hole configurations for bleed rates up to 12% of the boundary-layer mass flow rate.

2) The improved agreement for the shape of the predicted mean velocity distribution downstream of bleed band is attributed to including a history effect in the eddy viscosity model.

3) The Rotta-roughness formulation was an effective way to relate the equivalent sand-grain roughness height with the increase in the near-wall length scale for rough surfaces with and without mass bleed. Predicted momentum thicknesses agreed with the experimental data except where the boundary-layer developed under a strong adverse pressure gradient.

Further evaluation of the two-dimensional lag model based on experimental data for different freestream Mach number, upstream velocity profile shape, and bleed hole configuration conditions is recommended as test data becomes available. The model is intended for use in Navier-Stokes codes for analysis of supersonic inlet flows.

The success of the simple lag model suggests that an extension of a one-equation eddy viscosity model such as that under development by Spalart and Allmaras[5] may be desirable.

Acknowledgments

The 20- and 90-deg bleed hole data was obtained under NASA Contract NAS3-25963, "Bleed System Design Tech-

nology." The authors wish to thank the contract monitor, J. Wasserbauer of NASA Lewis Research Center for allowing the use of the data in this study.

References

[1]Paynter, G. C., Treiber, D. A., and Kneeling, W. D., "Modeling Supersonic Inlet Boundary-Layer Bleed Roughness," *Journal of Propulsion and Power*, Vol. 9, No. 4, 1993, pp. 622–627.

[2]Cebeci, T., and Chang, K. C., "Calculation of Incompressible Rough Wall Boundary Layer Flows," *AIAA Journal*, Vol. 16, No. 7, 1978, pp. 730–735.

[3]Reyhner, T. A., "Finite Difference Solution of the Compressible Turbulent Boundary Layer Equations," *Proceedings of Computation of Turbulent Boundary Layers—1968 AFOSR-IFP—Stanford Conference*, Vol. 1, 1968, pp. 375–383.

[4]Clauser, F. H., "The Turbulent Boundary Layer," *Advances in Applied Mechanics*, Vol. IV, Academic Press, Los Angeles, CA, 1956.

[5]Spalart, P. R., and Allmaras, S. R., "A One-Equation Turbulence Model for Aerodynamics Flows," AIAA Paper 92-0439, Jan. 1992.